Time-Course Changes in Speciation and Solubility of Cadmium in Reduced and Oxidized Paddy Soils

Mitsuhiro Furuya
Yohey Hashimoto*

Dep. of Bio-Applications
and Systems Engineering
Tokyo Univ. of Agriculture
and Technology
2-24-16 Naka-cho
Koganei, Tokyo 184-8588
Japan

Noriko Yamaguchi

Institute for Agro-environmental
Sciences
National Agriculture and
Food Research Organization
3-1-3 Kan-nondai
Tsukuba, Ibarkai 305-8604
Japan

A prolonged flooding during rice (*Oryza sativa* L.) cultivation is recommended to immobilize soil Cd by the formation of CdS under anoxic conditions. The problem with this recommended practice is that it reduces rice yields compared with intermittent flooding, which is less effective at immobilizing CdS through reductive precipitation. This study investigated the solubility of Cd in relation to chemical speciation of Cd and S and soil redox potential through a time series of measurements during a 29-d reduction period followed by a 20-d oxidation period using X-ray absorption fine structure spectroscopy and chemical extraction. Two Aquent soils with different S levels in water- and oxalate-extractable fractions (hereafter low-S and high-S soils) were used to investigate the formation and dissolution of CdS. In the reducing period, the CdS proportion in the high-S soil rapidly increased to 30% at Day 4 and reached 90% at Day 29, whereas CdS in the low-S soil did not exceed 35%. In the following oxidizing period, CdS in the soils underwent oxidative dissolution but was not completely dissolved, remaining at <20% of the total Cd. A two-piece segmented linear relationship existed between HCl-extractable Cd and soil Eh, and the regression slope was 28-fold greater for the low-S soil at Eh >435 mV and 38-fold greater for the high-S soil at Eh >529 mV. This result indicates that each soil has a threshold Eh value at which the solubility of Cd is drastically altered during the course of soil reduction and oxidation processes.

Abbreviations: EXAFS, extended X-ray absorption fine structure; LCF, linear combination fitting; XAFS, X-ray absorption fine structure; XANES, X-ray absorption near-edge structure.

C admium in paddy soils has long been recognized as a critical food safety problem in tropical and subtropical Asian countries where rice is an important staple in the human diet. Cadmium sulfide (solubility product constant $K_{sp} = 10^{-27}$) occurring in reduced soils is primarily attributed to the decrease in solubility of soil Cd (Cornu et al., 2007; de Livera et al., 2011; Huang et al., 2013). To minimize Cd uptake by rice plants, therefore, soil management practices have been focused on the enhancement of CdS formation in paddy soils. Keeping the soil flooded throughout the rice-growing period decreases the solubility of Cd and, as a result, decreases plant uptake of Cd. Hu et al. (2013b) and Inahara and Azuma (2007) reported that flooding the paddy soil before and after ear emergence of rice plants decreased the Cd concentration in brown rice compared with a control plot managed by intermittent irrigation. Arao et al. (2009) demonstrated that soil flooding decreased Cd concentrations in tissues and grains of rice plants, with a concomitant decrease in soil solution Cd. Such a decrease in Cd solubility in reduced soils was attributed to the probable transformation of soluble Cd species into CdS, although direct evidence using spectroscopic techniques have been little

Core Ideas

- The formation and dissolution of CdS were investigated in low- and high-S soils.

- CdS reached 90% in the high-S soil but did not exceed 35% in the low-S soil.

- Cd dissolved rapidly at soil Eh >435 mV (low-S soil) and >529 mV (high-S soil).

reported (Fulda et al., 2013; Hashimoto et al., 2016; Hashimoto and Yamaguchi, 2013; Khaokaew et al., 2011).

Recent investigations using synchrotron-based X-ray absorption fine structure (XAFS) spectroscopy directly determined chemical speciation of Cd in paddy soils (Fulda et al., 2013; Hashimoto et al., 2016; Hashimoto and Yamaguchi, 2013; Khaokaew et al., 2011). Three of these studies demonstrated that chemically extractable Cd in the reduced soils decreased with increasing proportions of CdS to the total Cd (Fulda et al., 2013; Hashimoto et al., 2016; Hashimoto and Yamaguchi, 2013). Solubility of Cd in soils is strongly associated with S dynamics. Fulda et al. (2013) revealed that the formation of CdS was inhibited in a soil with abundant Cu, which binds with sulfides more preferentially than Cd under reduced conditions, indicating the significance of competitive cations for CdS formation. In contrast, the formation of CdS increased more in a reduced soil amended with a greater amount of S impurities in zerovalent Fe powders (Hashimoto et al., 2016). The proportion of CdS was increased in a soil with a greater concentration of Mehlich-III and $NaHCO_3$–extractable SO_4 (Fulda et al., 2013; Hashimoto and Yamaguchi, 2013). Sulfate extracted by Mehlich-III and $NaHCO_3$ is considered to be associated mainly with soil minerals (Mehlich, 1984) and available for anaerobic microbial respiration (Lefroy et al., 1992), respectively. These studies suggest that not only the concentration factor but also the chemical speciation of S can be a determining factor controlling the formation of CdS in reduced soils.

A prolonged flooding during rice cultivation is recommended to enhance Cd immobilization via decreasing soil redox potential (Arao et al., 2009, 2010). However, continuous flooding in paddy soils retards root growth (Zhang et al., 2009) and grain yield (Hu et al., 2013a), and for better water management, intermittent irrigation has conventionally been practiced. Knowledge of the formation and dissolution of CdS along with redox gradients is therefore critical to be compatible with both Cd immobilization and plant growth. The objective of this study was to investigate the solubility of Cd in relation to chemical speciation of Cd and S during the time series of a 29-d reduction period and a following 20-d oxidation period using XAFS spectroscopy and chemical extraction. Very few studies have directly determined Cd speciation and hosting phases in anthropogenically contaminated soils (Khaokaew et al., 2011) or even in laboratory-spiked soils (Fulda et al., 2013; Hashimoto et al., 2016). In this study, Cd-spiked paddy soils with different S chemistry (water- and oxalate-extractable fractions) were compared to ascertain the

contiguous changes in CdS formation and dissolution during the course of reduction–oxidation processes.

MATERIALS AND METHODS
Soil Characterization

Two soils (Aquents) were collected from the plow layer of different paddy fields at the National Institute for Agro-environment Sciences, Tsukuba, Japan (hereafter NK soil), and FM Honmachi Field Science Center, Tokyo University of Agriculture and Technology (hereafter FM soil; Fuchu, Japan). These soils were not contaminated with Cd or other heavy metals and had different concentrations of water- and oxalate-extractable S (see Table 1). Basic soil physicochemical properties, such as texture, pH, elemental concentrations, water-extractable anions, acid ammonium oxalate Fe and Mn (Fe_{ox} and Mn_{ox}, respectively), and dithionite–citrate-extractable Fe and Mn (Fe_d and Mn_d, respectively) were determined by standard procedures. All chemicals used in this study were a special grade (>99% purity) purchased from Wako Pure Chemical Industries Ltd. unless otherwise noted.

Soil Incubation Experiment

An incubation experiment using Cd-spiked soils was conducted to asses Cd solubility and chemical speciation in relation to soil Eh. The soil incubation and soil Cd extraction were conducted at $25 \pm 1°C$ in the dark. The weight of soils added to 2.8-L containers (18-cm diameter, 14-cm length, and 2-mm thickness) was 1660 g for the NK soil and 1560 g for the FM soil. To enhance soil reduction during the incubation period, 1% (w/w) of powdered rice straw was added to the soils. To mimic Cd-contaminated soil, the soils were treated with $CdCl_2$ solution to achieve a Cd concentration of 150 mg kg^{-1}, and a homogenized soil slurry was prepared. For the first 29 d of the soil reducing period, the water levels were maintained at 2 cm above the soil surface by occasional additions of deionized water. Soil Eh and pH values at the depth of 7 cm were continuously measured by inserting a Pt electrode with a Ag/AgCl reference electrode and a thin glass electrode, respectively (DKK-TOA Corporation). About 2 g of soil was collected from the center of each soil column at Days 1, 3, 4, 5, 6, 8, 9, 19, and 29. At the end of the soil reducing period (Day 29), aliquots of soil (~80 mL each) were transferred to 10 polypropylene columns (6-cm diameter, 8-cm length, 2-mm thickness), and excess water was drained from the bottom of the column until Day 50 (oxidizing period). A Pt electrode and a Ag/AgCl reference electrode were installed for the

Table 1. Chemical properties of the FM and NK soils used in this study, including pH determined at a soil to water or 1 mol L^{-1} KCl ratio of 1:2.5, electrical conductivity determined at a soil/water ratio of 1:5, dithionite-citrate extractable Fe and Mn acid (crystalline and poorly-crystalline phases) (Fe$_d$ and Mn$_d$, respectively), acid ammonium oxalate extractable Fe and Mn (poorly crystalline phase) (Fe$_{ox}$ and Mn$_{ox}$, respectively), SO$_4$ extracted by water for 1 h at a soil/water ratio of 1:50, and acid ammonium oxalate extractable S (S$_{ox}$).

Soil	pH (H$_2$O)	pH (KCl)	EC	Sand	Silt	Clay	Total C	Total N	Fe$_d$	Fe$_{ox}$	Mn$_d$	Mn$_{ox}$	Total Zn	SO$_4$	S$_{ox}$
			dS m^{-1}				g kg^{-1}							mg kg^{-1}	
FM	6.7	5.7	0.10	362	309	184	49.7	3.6	15.1	5.5	0.05	0.04	114	120	253
NK	5.7	4.6	0.07	398	228	374	21.2	2.5	16.9	7.3	0.17	0.15	57	72	89

soil Eh measurement (Fujiwara Co.). Up to Day 50, the columns were periodically dismantled, and the soil samples were collected from the column center.

Soil Cd was immediately extracted with 0.1 mol L^{-1} HCl solution with a soil/solution ratio of 1:100 (0.3 g/30 mL) for 2 h ($n = 3$). Prior to the extraction process, excess water in the soil was removed by centrifugation (4 min at 470 × g). The soil extract was passed through a 0.45-μm membrane filter and analyzed for Cd by atomic absorption spectroscopy (Z-5010, Hitachi High-Technologies Co. Ltd.). The Cd concentrations based on the weight of soil were corrected for water content. Aliquots of soils were immediately vacuum sealed with deoxidants (AGELESS, Mitsubishi Gas Chemical Company) and stored at −80°C for Cd XAFS analysis, and freeze-dried for S X-ray absorption near-edge spectroscopy (XANES) analysis.

Cadmium and Sulfur K-edge XAFS Spectroscopy

Speciation of Cd in selected soil samples from the reducing period (Days 1, 4, 19, and 29) and oxidizing period (Days 34, 36, 39, 41, 45, and 50) were analyzed for Cd K-edge XAFS spectroscopy at Beamline BL01B1 at SPring-8 in Hyogo, Japan. The Cd reference compounds used for the following linear combination fitting (LCF) procedure were reported in our previous study (Hashimoto et al., 2016), including $CdCO_3$, $Cd(NO_3)_2$, $CdCl_2$, $CdSO_4$, $Cd(OH)_2$, $Cd(CH_3COO)_2$, CdS (>99.9% purity, purchased from Kanto Kagaku Ltd.), and Cd sorbed on ferrihydrite, birnessite, humus, and phyllosilicate (kaolinite). The purchased Cd compounds were diluted with BN to a Cd concentration of 10% (w/w) and pressed into pellets with 10-mm diameter and 1-mm thickness. The synthesized Cd references were vacuum or freeze-dried and homogenized using mortar and pestle. The XAFS data were collected in transmission mode for BN-diluted references and in fluorescent mode with a 19-element Ge semiconductor detector for synthesized references and soil samples at ambient temperature across the Cd K absorption edge at 26,711 eV using Si (311) monochromator crystals. Energy calibration was made by the white line peak of CdO assigned at 26,711 eV.

Background correction, normalization, and conversion to k-space were performed on the data for Cd K-edge extended X-ray absorption fine structure (EXAFS) using the program Athena Version 0.9.22 (Ravel and Newville, 2005). Fourier transformation of the k^3–weighted $\chi(k)$ function was performed to obtain a radial structure function. The LCF procedure with binary combinations of Cd references was used to determine the relative proportions of Cd species in the multicomponent EXAFS spectra of soil samples. The quality of the LCF result was quantified by estimating the residual (R) value, defined as

$$R = \frac{\sum \left(\mu_{exp} - \mu_{model} \right)^2}{\sum \left(\mu_{exp} \right)^2}$$

where μ is the normalized absorption. Among all references, the binary-component fit resulting in the best R value is reported. Also, the results of the second-best fit, which are shown similarly

to those of the best fit, are reported in Supplemental Table S1. This LCF procedure can avoid non-unique fitting solutions because the use of a large number of references can inappropriately improve the R value (Hashimoto et al., 2011; Hashimoto and Yamaguchi, 2013). The quality of the LCF result was quantified as a residual (R) value (see supplemental material). All LCF values on k^3–weighted EXAFS spectra were determined in the energy range between 2.0 and 7.5 Å^{-1}. Due to a limited beam-time and spectrum quality, the LCF for the EXAFS spectra was performed on a relatively narrow range of k space; therefore, we aimed primarily at the determination of CdS in the soil samples using the LCF on the EXAFS spectra.

The Cd K-edge XANES data were background corrected and normalized using the same software program. To confirm the results of the EXAFS–LCF, the relative proportions of Cd species in the multicomponent XANES spectra of the soil samples were obtained by the LCF procedure using all possible binary combinations of Cd references. All LCFs were performed in the energy range between 26,691 and 26,761 eV (i.e., relative energy between −20 and 50 eV).

Speciation of S in selected soil samples from the reducing period (Days 1 and 29) and oxidizing period (Days 34, 36, 39, and 50) were analyzed by S K-edge XANES on Beamline BL11B at the Photon Factory in Tsukuba, Japan. Reference S compounds used included ones with an oxidation state between −2 and +6, which were also reported in our previous study (Hashimoto and Yamaguchi, 2013). Sulfur K-edge XANES data were collected in a total electron yield mode for reference materials and in fluorescent mode for soil samples at ambient temperature under a vacuumed condition. The data were collected with stepwise 0.2-eV increments with 2 s per point from 2455 to 2500 eV and in 0.25-eV increments with 2 s per point from 2500 to 2530 eV. The S K-edge XANES data were calibrated using the first inflection point of the most intense peak of sodium dodecyl sulfate (S^{VI}), set to 2472.5 eV, and processed for background correction and normalization using the program Athena Version 0.9.22.

RESULTS
Soil Characterization

Table 1 shows the physicochemical properties of the NK and FM soils. The pH value of the FM soil (6.7) was one unit greater than that of the NK soil (5.7). According to the USDA soil texture system, the NK and FM soils were classified as clay loam and loam, respectively. Total C and Zn contents in the FM soil (49.7 g kg^{-1} and 114 mg kg^{-1}) were twice those in the NK soil (21.2 g kg^{-1} and 57 mg kg^{-1}). Water-extractable SO_4^{2-} in the FM soil (120 mg kg^{-1}) was greater than in the NK soil (72 mg kg^{-1}). It is noteworthy that oxalate-extractable S was markedly greater in the FM soil (253 mg kg^{-1}) than the NK soil (89 mg kg^{-1}). The oxalate fluid selectively extracts short-range-order minerals including Fe (oxy)hydroxides, and therefore S associated with those minerals may dissolve in reduced soils via reductive-dissolution reactions.

Soil Redox Potential

Figure 1 shows the changes in Eh values of the soils during the 29-d reducing period followed by the 20-d oxidizing period. A horizontal dotted line at the Eh value of -75 mV in Fig. 1 indicates the threshold Eh value at which soil Cd starts to precipitate as CdS in the presence of stoichiometrically sufficient SO_4^{2-} (1 mmol L^{-1}) at pH 6 (Lindsay, 1979). The soil redox potential decreased more rapidly in the FM than the NK soils during the reducing period. The period required for the soil Eh to reach the critical value (-75 mV) for CdS formation was 3 d for the FM soil and 8 d for the NK soil. The Eh values of the NK soil hovered around -100 mV until Day 19 and thereafter decreased to -200 mV by Day 27. Compared with the NK soil, the redox status was more anoxic in the FM soil, where the Eh values remained constant below -200 mV from Days 14 to 29. After the water was drained from both soils on Day 29, the soil Eh value rose rapidly to 0 mV. The redox status of the FM and NK soils reached oxic levels around 500 mV by Day 34 and thereafter.

Cadmium Solubility and Redox Potential

Figure 2a shows the concentration of Cd extracted by 0.1 mol L^{-1} HCl as a function of the soil incubation period. Extractable Cd concentrations in the NK soil were greater than those of the FM soil during the reducing period (Days 0–29). During the reducing period, Cd concentrations decreased from 110 to 95 mg kg^{-1} in the NK soil and from 96 to 70 mg kg^{-1} in the FM soil. In the oxidizing period from Day 29, extracted Cd concentrations of both soils rapidly increased during the first 10 d ($\sim$Day 40) and reached 144 mg kg^{-1} at Day 50. Figure 2b illustrates the HCl-extracted Cd concentration of the soils as a function of soil Eh values during the incubation period. Extractable Cd concentrations in the NK soil were overall greater than those in the FM soil throughout the soil incubation period. Extracted Cd concentrations decreased with decreasing Eh values for both soils. A threshold Eh value determined by the intersection of two linear regression models between Cd concentration and Eh was greater in the FM soil (529 mV) than the NK soil (441 mV). In

the NK soil, the slope of the linear regression for Eh against Cd concentration was 0.01 at Eh < 441 mV and 0.28 at Eh > 441 mV, illustrating that the solubility of Cd was 28-fold greater at Eh > 441 mV. Similarly, the solubility of Cd in the FM soil was increased to 38-fold at Eh > 529 mV. This result indicates that each soil has a threshold Eh value at which the solubility of Cd is drastically altered during the course of soil reduction and oxidation processes.

Cadmium and Sulfur K-edge XAFS Spectroscopy

Cadmium K-edge EXAFS spectra for selected references and soil samples are shown in Fig. 3. The reference for CdS and other compounds having a Cd–O bond in the first shell can be distinguished by the position of the first oscillation that is shifted to a greater k for CdS ($\sim$4 Å^{-1}) than the others ($\sim$3.5 Å^{-1}). According to visual observations, the EXAFS spectra of the soil samples were similar to those of Cd associated with soil colloids
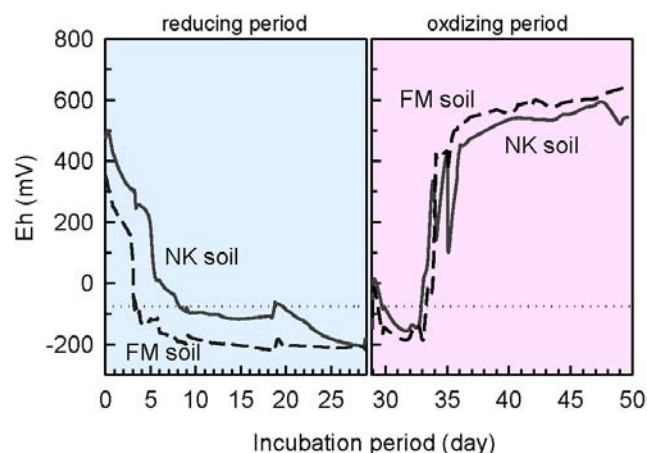

Fig. 1. The Eh values of the soils in the reducing and oxidizing periods. The solid and broken lines indicate the Eh values for the NK and FM soils, respectively. The horizontal dotted lines at Eh = -75 mV indicate that CdS precipitates occurred below this level at pH 6.
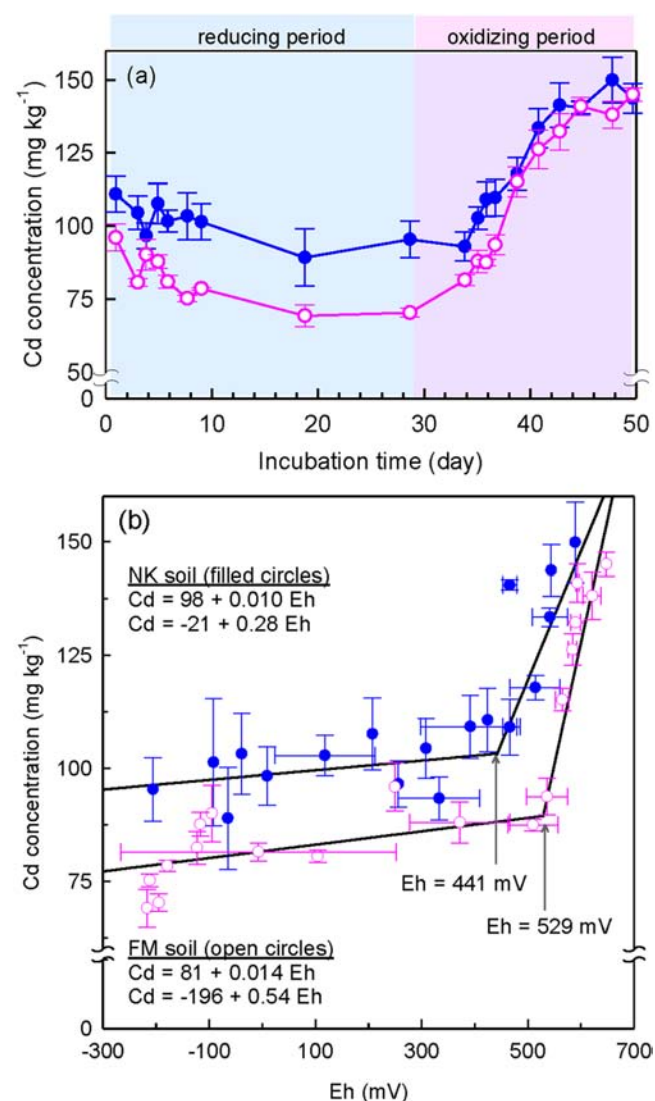

Fig. 2. The HCl-extracted Cd concentration as a function of (a) soil incubation period and (b) soil Eh for the FM and NK soils. Error bars represent standard deviations of the mean. Nonlinear regression determined the breakpoint between Cd concentration and Eh using the PROC NLIN procedure in SAS Version 9.2.
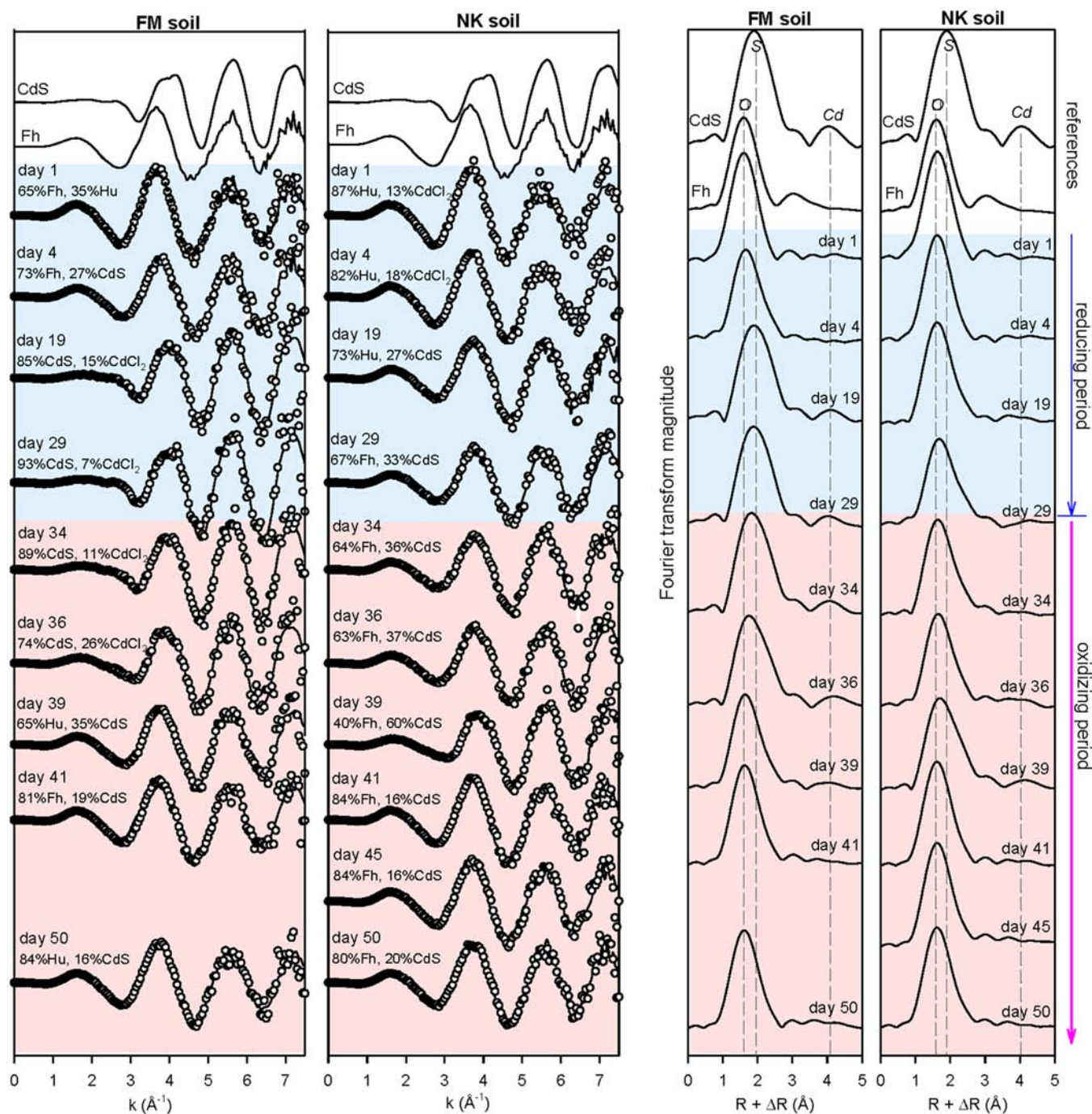
Fig. 3. The k^3–weighted Cd K-edge extended X-ray absorption fine structure (EXAFS) spectra of reference compounds and soil samples (left, circles) and their linear combination fitting using the reference spectra (right, solid lines) and Fourier-transform magnitudes of EXAFS spectra for reference compounds and soil samples. Fh: Cd sorbed with ferrihydrite; Hu: Cd sorbed with humus.

(i.e., ferrihydrite and humus) at the early stage of the reducing period, and they became similar to the CdS reference spectrum toward the end of the reducing period at Day 29. In the following oxidizing period up to Day 50, the overall curvature of the soil EXAFS spectra was changed from CdS to Cd–ferrihydrite and –humus references, implying the occurrence of oxidative dissolution of CdS. These features in k^3–weighted EXAFS spectra were also confirmed in Fourier-transformed EXAFS spectra (Fig. 3), which contained peaks reflecting the relative radial distance between the central Cd and neighboring atoms. The first shell of the FM soil sample corresponded to that of a Cd–O bond

($\sim$1.5 Å) in the early stage of the reducing period (Days 1 and 4). In the process of soil reduction and subsequent soil oxidation (up to Day 36), the first shell of the FM soil samples corresponded to that of a Cd–S bond for CdS ($\sim$2.0 Å), and the second shell indicative of a Cd–Cd bond ($\sim$4.0 Å) in CdS was also observed. These features of radial structure function allow determination of the formation and dissolution of CdS as a function of soil redox potential.

For more quantitative determination of Cd species in a series of reduction–oxidation periods, EXAFS–LCF was per-

formed on the soil spectra using Cd reference spectra (Fig. 4a). During the reducing period, the CdS proportion in the FM soil increased gradually and reached 93% at Day 29. During the oxidizing period from Day 30, the proportion of CdS in the FM soil decreased rapidly to 19% at Day 41 and remained unchanged until the end of the oxidation period at Day 50. The CdS proportion of the NK soil increased constantly during the reducing period, but it did not exceed 33% of the total Cd in the soil. During the following oxidizing period, the proportion of CdS decreased to 20% until Day 41. The proportion of soil CdS determined by EXAFS–LCF was consistent overall with that determined by XANES–LCF (Supplemental Table S2). The proportions of soil CdS determined by EXAFS– and XANES–LCF had a negative linear relationship with the concentrations of HCl-extractable Cd (Fig. 4b and 4c). The slope of the linear regression of CdS

proportions against acid-extractable Cd concentrations was −0.31 during the reducing period and −0.80 during the oxidizing period, illustrating about a 2.5-fold difference in the regression slopes. This result indicates that the decrease in Cd solubility is closely related to the increase in the CdS proportion of the total Cd in the soil, and the solubility of Cd increases more during the soil oxidizing than reducing periods due to oxidative dissolution of CdS.

Figure 5 shows the proportion of S species groups as a function of the soil incubation period. The oxidized S group in the FM soil decreased from 60 to 44% during the reducing period. During the following oxidizing period, the oxidized S group increased to 66% at Day 36. This increase in oxidized S during the initial stage of soil oxidation corresponded to the rapid decrease in CdS in the FM soil (Fig. 4a). After Day 36, the proportions of oxidized S groups, along with CdS, remained constant at around 60 and 20%, respectively (Fig. 4a). The same trend in S species was observed in the NK soil during the reducing period, when the oxidized S group decreased from 88 to 72%. During the soil reducing period, the proportion of oxidized S groups in the NK soil ranged from 70 to 80%, and the proportion of reduced S groups peaked at 11% on Day 34 and decreased thereafter with increasing soil redox potential.

DISCUSSION

Our study found a contrasting difference in the formation of CdS between the FM and NK soils during the reducing period. During the 29-d reduction period, the proportion of CdS reached 93% in the FM soil and 33% in the NK soil (Fig. 3 and 4a). One of the critical factors regulating the formation of CdS is the nature of S in the soil. A considerably greater amount of
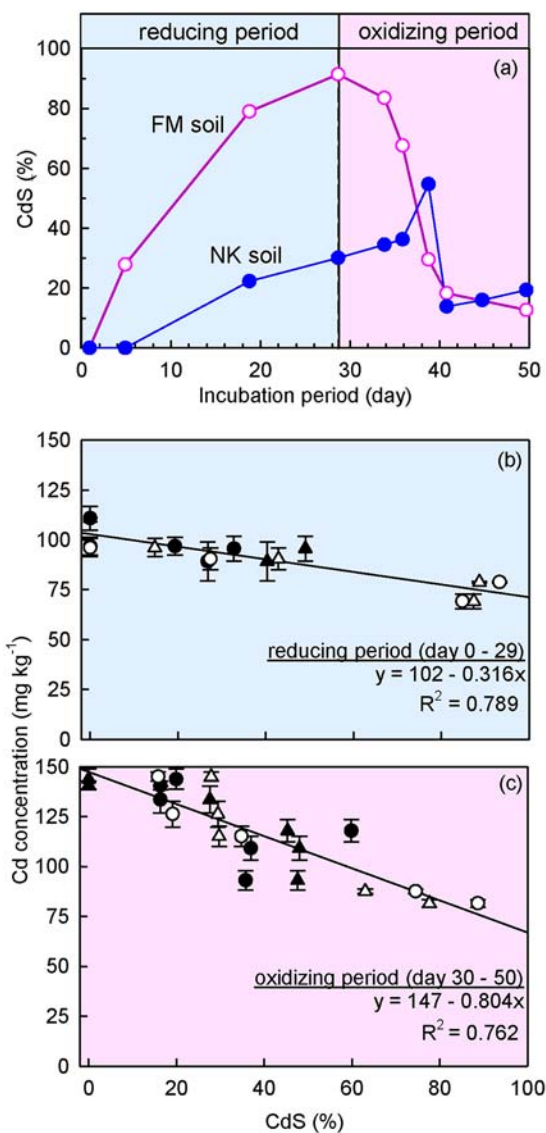

Fig. 4. (a) The proportion of CdS derived from extended X-ray absorption fine structure (EXAFS)–linear combination fitting (LCF) as a function of soil incubation period in FM (open circles) and NK (filled circles) soils and the 0.1 mol L⁻¹ HCl extracted Cd concentration as a function of the proportion of CdS derived from EXAFS–LCF (circles) and X-ray absorption near-edge spectroscopy (XANES)–LCF (triangles) in the (b) reducing period and (c) oxidizing period.
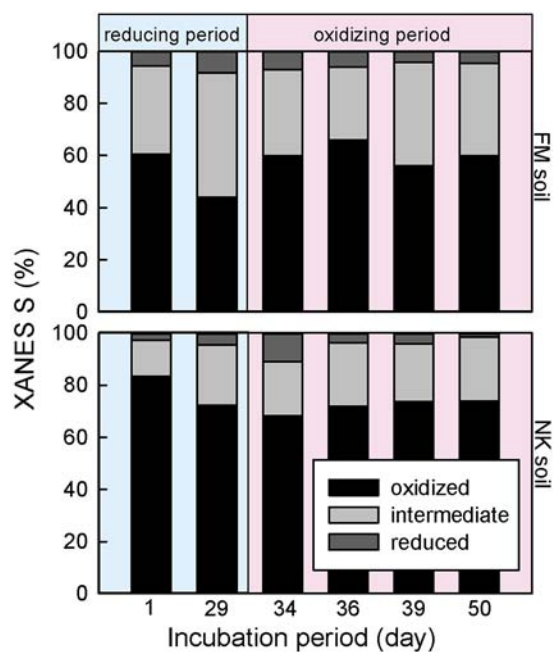

Fig. 5. The proportion of grouped S species from the X-ray absorption near-edge spectroscopy (XANES) peak fit as a function of incubation period. Sulfur species are grouped into reduced, intermediate, and oxidized forms according to their oxidation states.

oxalate-extractable S was found in the FM soil (253 mg kg^{-1}) than the NK soil (89 mg kg^{-1}; Table 1). Acid ammonium oxalate is known to extract short-range-order minerals (e.g., ferrihydrite) and can dissolve organic S (Tanikawa et al., 2009, 2014) and sulfate associated with nanocrystalline minerals (Parfitt and Childs, 1988). In the process of reduction, soil S associated with redox-sensitive minerals is liberated via reductive dissolution, which may result in the increased formation of CdS in the FM soil (93%) more than the NK soil (33%) (Fig. 4a). In addition to the oxalate-extractable S, the FM soil had a greater concentration of water-extractable SO$_4$ than in the NK soil (Table 1). The difference in the concentration of readily soluble SO$_4$ may be attributed to the difference in the kinetics of CdS formation in the early stage of the soil reduction process. This is demonstrated by the result of XAFS–LCF, showing that the proportion of CdS on Day 4 was increased to 30%, but CdS was not detected in the NK soil (Fig. 4a).

It has been reported that the proportion of CdS under anoxic conditions increased more in a soil with greater S contents extracted by Mehlich-III (Hashimoto and Yamaguchi, 2013) and NaHCO$_3$ (Fulda et al., 2013). Hashimoto et al. (2016) used micro-focused X-ray fluorescence and XANES spectroscopy to investigate the formation of CdS at soil microsites and revealed that the addition of zerovalent Fe powder with greater S contents increased CdS and dissolved SO$_4$ in a reduced soil. In contrast, the process of CdS formation slowed in a soil with low S contents, where the CdS proportion reached <0% of the total Cd. Our study suggests that (i) the amount of S in the water-soluble fraction is related to the kinetics of CdS formation in the initial stage of soil reduction, and (ii) the amount of S in the redox-sensitive mineral fraction, which is assumed to be extracted by ammonium oxalate, may determine the potential of CdS formation in the reduced soil.

The oxidation state of S is another critical factor determining the formation of CdS in anoxic soils. Transformation of sulfate (S^{VI}) into sulfide (S^{-II}) in the soil reduction process is a prerequisite to drive the chemical reaction to form CdS in the soil. During the entire soil incubation period, the proportions of CdS and reduced S species were greater in the FM soil than the NK soil (Fig. 4 and 5). The Cd and S K-edge XAFS study revealed that the proportions of CdS showed a positive correlation with those of reduced S species ($r = 0.70$, Fig. 6a) and a negative correlation with those of oxidized S species ($r = -0.50$, Fig. 6c). These

results provide direct evidence demonstrating the contribution of reduced S species to the formation of CdS in the soil. The mineralization rate of organic S, which eventually increases the levels of reduced sulfide in anoxic soils, may also affect the CdS precipitation reaction, although this remains unclear.

The enhanced formation of CdS in the FM soil compared with the NK soil was also attributed to the decrease in redox potential, which occurred more rapidly in the FM than the NK soil during the reducing period. Our study found that the period of time required for the soil Eh value to decrease below the critical point for CdS formation (−75 mV at pH 6) was 3 d for the FM soil and 8 d for the NK soil (Fig. 1a). Corresponding to the rapid decrease in Eh for the FM soil, about 30% of the soil Cd was transformed into CdS by Day 4, whereas CdS was not detected in the NK soil (Fig. 4a). These results, based on the molecular spectroscopic investigation, agreed with those based on the prediction using an Eh–pH diagram (Supplemental Fig. S1). Compared with the NK soil, a rapid decrease in the soil redox potential in the FM soil was explained by a greater amount of organic C (Table 1), which generally accelerates the soil reduction process (Kashem and Singh, 2001; Yagi and Minami, 1990)

The dissolution process of CdS in the FM soil proceeded more rapidly than in the NK soil during the oxidizing period from Day 29 and thereafter (Fig. 4a). During the initial 10 d of the oxidizing period, the proportion of CdS decreased from 93 to 35% in the FM soil, whereas such rapid decrease in CdS was not found in the NK soil. The rapid dissolution of CdS in the FM soil was also confirmed by the increase in acid-extractable Cd (Fig. 2a), which may be attributed to the fast oxidation process in the beginning of the oxidizing period (Days 29–35). This can be explained by the elevation of the soil Eh value, which rose to 450 mV in the FM soil but stayed low at around 200 mV in the NK soil. The NK soil with abundant clay contents (374 g kg^{-1}) relative to the FM soil (184 g kg^{-1}) could increase water retention, which probably retarded the soil oxidation process and sequestered CdS from oxidative dissolution.

CONCLUSIONS AND IMPLICATIONS

In summary, the Cd-XAFS results provide one explanation for how the decrease in acid-extractable Cd relates to the increase in CdS in the soil. Acid-extractable Cd decreased with the increasing proportion of CdS during the reducing and oxidizing periods, and Cd solubility with respect to CdS was 2.5-fold
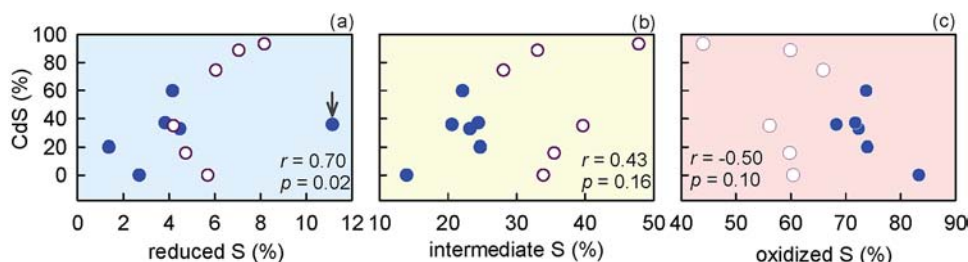

Fig. 6. The proportion of CdS derived from extended X-ray absorption fine structure (EXAFS)–linear combination fitting as a function of (a) reduced S, (b) intermediate S, and (c) oxidized S in FM (open circles) and NK (filled circles) soils. Sulfur species are grouped into reduced, intermediate, and oxidized forms in accordance to their oxidation states. The plot with an arrow in (a) was excluded from Pearson's correlation analysis.

greater during the oxidizing than the reducing periods (i.e., slope in Fig. 4b and 4c). The two-segment regression on acid-extractable Cd and Eh during the course of the reduction and oxidation periods determined that Cd solubility increased drastically when the soil Eh value exceeded 441 mV for the NK soil and 529 mV for the FM soil (Fig. 2b). Such threshold values for Cd solubility were not determined when pH was used as a predictor value of soil extractable Cd throughout the reduction–oxidation period (Supplemental Fig. S2), attesting that the solubility of Cd in the redox soil system is chiefly controlled by CdS.

Numerous studies have reported the effectiveness of prolonged flooding on reducing Cd uptake by rice plants (Arao et al., 2009, 2010; Bingham et al., 1976; Hu et al., 2013a). To the contrary, continuous flooding caused a loss of grain yield for some rice cultivars (Hu et al., 2013a). Thus, a conflict exists between creating soil conditions that promote optimal yield and maximize Cd immobilization. To achieve both a reduction in Cd uptake and an increase in the grain yield, therefore, the optimal duration of flooding may be judiciously determined by measuring the soil Eh value, which allows continuous monitoring of soil conditions at the field level. It should be noted that the threshold Eh value for determining the change in Cd solubility may vary depending on soil physical and chemical properties, including presumably the water holding capacity and clay and C contents.

SUPPLEMENTAL MATERIAL

The supplemental material includes an Eh–pH diagram for Cd speciation in the soil solution, acid-extractable Cd as a function of soil pH, and soil Cd and S K-edge XAFS spectra and their LCF results.

REFERENCES

Arao, T., S. Ishikawa, M. Murakami, K. Abe, Y. Maejima, and T. Makino. 2010. Heavy metal contamination of agricultural soil and countermeasures in Japan. Paddy Water Environ. 8:247–257. doi:10.1007/s10333-010-0205-7

Arao, T., A. Kawasaki, K. Baba, S. Mori, and S. Matsumoto. 2009. Effects of water management on cadmium and arsenic accumulation and dimethylarsinic acid concentrations in Japanese rice. Environ. Sci. Technol. 43:9361–9367. doi:10.1021/es9022738

Bingham, F.T., A.L. Page, R.J. Mahler, and T.J. Ganje. 1976. Cadmium availability to rice in sludge-amended soil under flood and non-flood culture. Soil Sci. Soc. Am. J. 40:715–719. doi:10.2136/sssaj1976.03615995004000050030x

Cornu, J.Y., L. Denaix, A. Schneider, and S. Pellerin. 2007. Temporal evolution of redox processes and free Cd dynamics in a metal-contaminated soil after rewetting. Chemosphere 70:306–314. doi:10.1016/j.chemosphere.2007.06.003

de Livera, J., M.J. McLaughlin, G.M. Hettiarachchi, J.K. Kirby, and D.G. Beak. 2011. Cadmium solubility in paddy soils: Effects of soil oxidation, metal sulfides and competitive ions. Sci. Total Environ. 409:1489–1497. doi:10.1016/j.scitotenv.2010.12.028

Fulda, B., A. Voegelin, and R. Kretzschmar. 2013. Redox-controlled changes in cadmium solubility and solid-phase speciation in a paddy soil as affected by reducible sulfate and copper. Environ. Sci. Technol. 47:12775–12783. doi:10.1021/es401997d

Hashimoto, Y., M. Furuya, N. Yamaguchi, and T. Makino. 2016. Zerovalent iron with high sulfur content enhances the formation of cadmium sulfide in reduced paddy soils. Soil Sci. Soc. Am. J. 80:55–63. doi:10.2136/sssaj2015.06.0217

Hashimoto, Y., M. Takaoka, and K. Shiota. 2011. Enhanced transformation of lead speciation in rhizosphere soils using phosphorus amendments and phytostabilization: XAFS spectroscopy investigation. J. Environ. Qual. 40:696–703. doi:10.2134/jeq2010.0057

Hashimoto, Y., and N. Yamaguchi. 2013. Chemical speciation of cadmium and sulfur K-edge XANES spectroscopy in flooded paddy soils amended with zerovalent iron. Soil Sci. Soc. Am. J. 77:1189–1198. doi:10.2136/sssaj2013.01.0038

Hu, P.J., J.X. Huang, Y.N. Ouyang, L.H. Wu, J. Song, S.F. Wang, et al. 2013a. Water management affects arsenic and cadmium accumulation in different rice cultivars. Environ. Geochem. Health 35:767–778. doi:10.1007/s10653-013-9533-z

Hu, P.J., Z. Li, C. Yuan, Y.N. Ouyang, L.Q. Zhou, J.X. Huang, et al. 2013b. Effect of water management on cadmium and arsenic accumulation by rice (*Oryza sativa* L.) with different metal accumulation capacities. J. Soils Sediments 13:916–924. doi:10.1007/s11368-013-0658-6

Huang, J.H., S.L. Wang, J.H. Lin, Y.M. Chen, and M.K. Wang. 2013. Dynamics of cadmium concentration in contaminated rice paddy soils with submerging time. Paddy Water Environ. 11:483–491. doi:10.1007/s10333-012-0339-x

Inahara, M.Y.O., and H. Azuma. 2007. Countermeasure by means of flooding in latter growth stage to restrain cadmium uptake by lowland rice. (In Japanese with English abstract.) Jpn. J. Soil Sci. Plant Nutr. 78:149–155.

Kashem, M.A., and B.R. Singh. 2001. Metal availability in contaminated soils: I. Effects of flooding and organic matter on changes in Eh, pH and solubility of Cd, Ni and Zn. Nutr. Cycling Agroecosyst. 61:247–255. doi:10.1023/A:1013762204510

Khaokaew, S., R.L. Chaney, G. Landrot, M. Ginder-Vogel, and D.L. Sparks. 2011. Speciation and release kinetics of cadmium in an alkaline paddy soil under various flooding periods and draining conditions. Environ. Sci. Technol. 45:4249–4255. doi:10.1021/es103971y

Lefroy, R.D.B., C.P. Mamaril, G.J. Blair, and P.J. Gonzales. 1992. Sulphur cycling in rice wetlands. In: R.W. Howarth et al., editors, Sulphur cycling on the continents: Wetlands, terrestrial ecosystems and associated water bodies. John Wiley & Sons Ltd., Chichester, UK. p. 279–300.

Lindsay, W.L. 1979. Chemical equilibria in soils. John Wiley & Sons, New York.

Mehlich, A. 1984. Mehlich 3 soil test extractant: A modification of Mehlich 2 extractant. Commun. Soil Sci. Plant Anal. 15:1409–1416. doi:10.1080/00103628409367568

Parfitt, R.L., and C.W. Childs. 1988. Estimation of forms of Fe and Al: A review, and analysis of contrasting soils by dissolution and Mossbauer methods. Aust. J. Soil Res. 26:121–144. doi:10.1071/SR9880121

Ravel, B., and M. Newville. 2005. ATHENA, ARTEMIS, HEPHAESTUS: Data analysis for X-ray absorption spectroscopy using IFEFFIT. J. Synchrotron Radiat. 12:537–541. doi:10.1107/S0909049505012719

Tanikawa, T., Y. Hashimoto, N. Yamaguchi, Y. Ito, S. Fukushima, K. Kanda, et al. 2014. Sulfur accumulation in Melanudands during development by upbuilding pedogenesis since 14–15 cal. ka. Geoderma 232–234:609–618. doi:10.1016/j.geoderma.2014.06.013

Tanikawa, T., M. Takahashi, A. Imaya, and K. Ishizuka. 2009. Highly accumulated sulfur constituents and their mineralogical relationships in Andisols from central Japan. Geoderma 151:42–49. doi:10.1016/j.geoderma.2009.02.025

Yagi, K., and K. Minami. 1990. Effect of organic matter application on methane emission from some Japanese paddy fields. Soil Sci. Plant Nutr. 36:599–610. doi:10.1080/00380768.1990.10416797

Zhang, H., Y.G. Xue, Z.Q. Wang, J.C. Yang, and J.H. Zhang. 2009. An alternate wetting and moderate soil drying regime improves root and shoot growth in rice. Crop Sci. 49:2246–2260. doi:10.2135/cropsci2009.02.0099

Supplemental Material

Time-course changes in speciation and solubility of Cd in reduced and oxidized paddy soils

Mitsuhiro Furuya[1], Yohey Hashimoto*[1], and Noriko Yamaguchi[2]

1) Tokyo University of Agriculture and Technology
2) National Agriculture and Food Research Organization

*CORRESPONDING AUTHOR
Tokyo University of Agriculture and Technology
2-24-16 Naka-cho, Koganei, Tokyo, 184-8588 Japan
E-mail: yhashim@cc.tuat.ac.jp

- Number of pages: 7

- Number of figures: 4

- Number of tables: 2

An Eh-pH diagram for Cd speciation in the soil solution
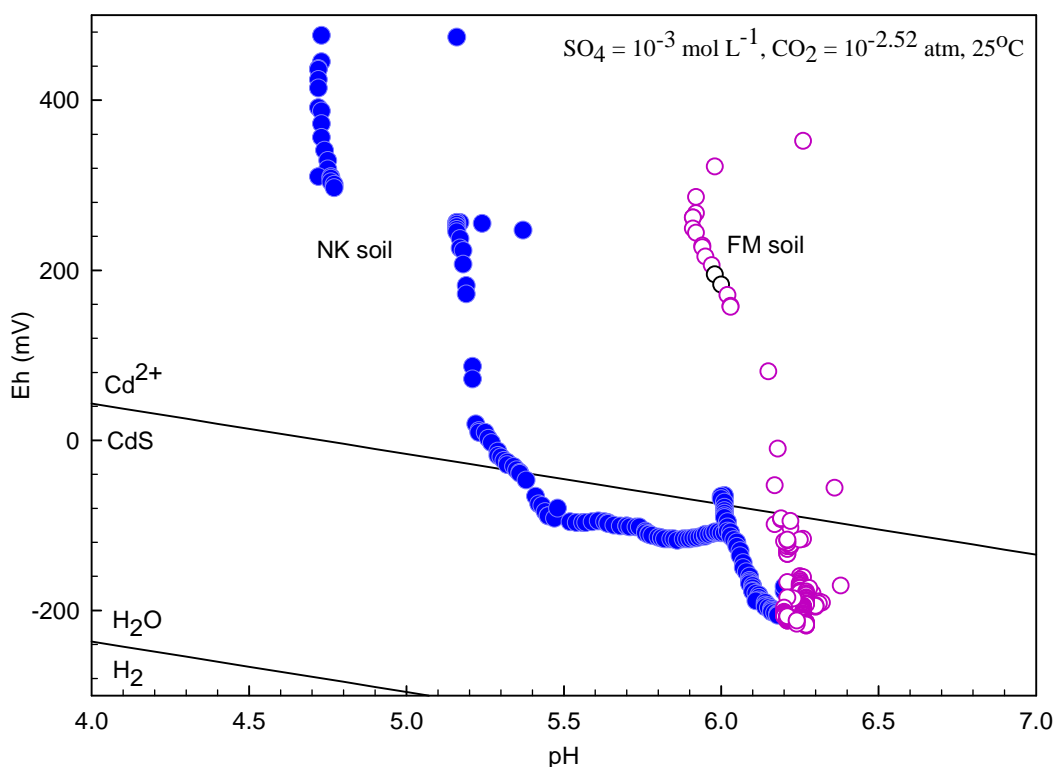
Fig. S1. Redox speciation of Cd in NK (filled circles) and FM (open circles) soil in the reducing period. The voltage measured in the soil is converted to one standardize with a hydrogen electrode using the following equation at 25 ^oC: Eh = V + 206; where Eh (mV) is the corrected redox potential, V (mV) is the voltage measured in the soil.

The equilibrium reactions and equilibrium constants (*log K*) of Cd species were based on Lindsay (1979):

$$Soil\text{-}Cd \leftrightarrow Cd^{2+} \quad (-7.00)$$
$$Cd^{2+} + S^{2-} \leftrightarrow CdS \quad (27.07)$$
$$SO_4^{2-} + 8e^- + 8H^+ \leftrightarrow S^{2-} + 4H_2O \quad (20.74)$$
$$Cd^{2+} + CO_2 + H_2O \leftrightarrow CdCO_3^0 + 2H^+ \quad (-14.06)$$
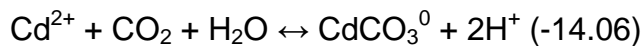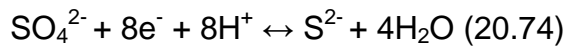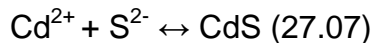
HCl extracted Cd in relation to soil pH

Soil Cd was immediately extracted with 0.1 mol L^{-1} HCl solution with a soil/solution ratio of 1:100 (0.3 g/30 mL) for 2 h (n = 3). Prior to the extraction process, excess water in the soil was removed by centrifugation (4 min at 470 g), but was not completely removed. The concentrations of Cd based on the weight of soil were corrected for water content (60%) for all soils. The concentrations of HCl-extracted Cd tend to increase with decreasing soil pH during the reducing period (a) whereas such relationship is little found in the soil during the oxidizing period (b).
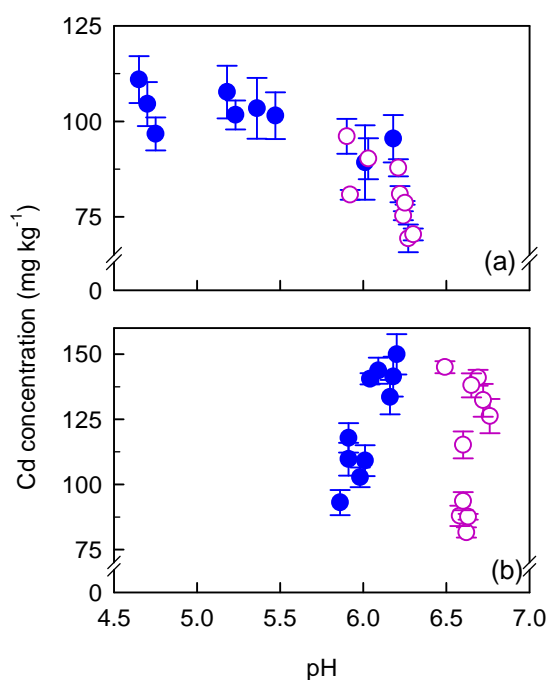

Fig. S2. 0.1 M HCl extracted Cd concentration as a function of soil pH in the reducing period (a) and oxidizing period (b) in FM (open circle) and NK (filled circle) soils. Error bars represent standard deviations of mean.

Cd K-edge XANES spectroscopy

The Cd K-edge XANES spectra have an absorption edge at ~26,715 eV (Fig. S3). The spectrum of CdS is characterized by a flat shoulder at the post-edge range whereas the spectrum of Cd associated with ferrihydrite (Cd-O) has a relatively high absorption value. As previously reported (Hashimoto and Yamaguchi, 2013), such differences in the XANES spectra can be used to distinguish CdS (Cd-S bond) from other Cd associated with soil colloids (Cd-O bond). According to visual observations, the XANES spectrum of soil samples were similar to that of Cd-soil reference at the early stage of reducing period, and then became similar to that of CdS reference toward the end of reducing period at day 29. In the following oxidizing period up to day 50, the shape of soil XANES spectra was shifted from the CdS to Cd-O references.
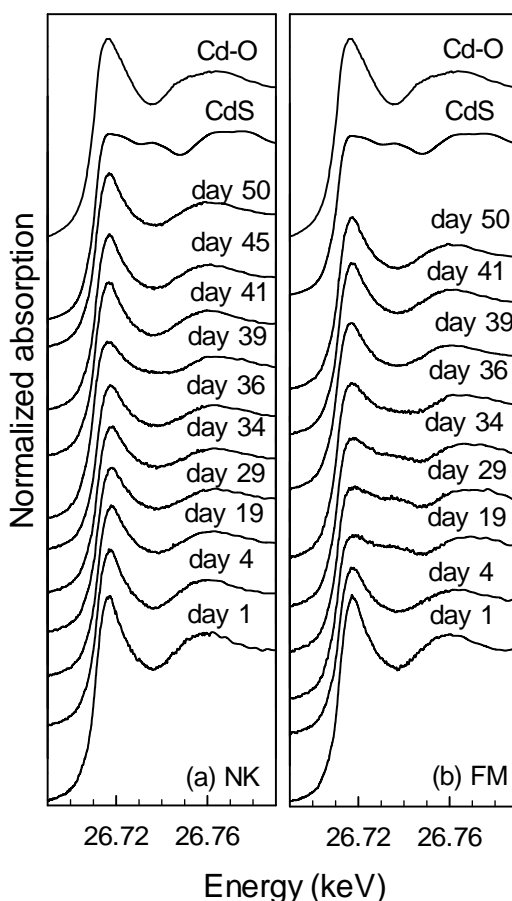
Fig. S3. Normalized Cd K-edge XANES spectra of NK soil (a) and FM soil (b) in the reducing (day 1-29) and oxidizing periods (day 34 and thereafter).

S K-edge XANES spectroscopy

Figure S4 shows S K-edge XANES spectra of (a) FM and (b) NK soil samples. These spectra were characterized by multiple white-line peaks, derived from multiple oxidation states of soil S. According to the previous study (Hashimoto and Yamaguchi, 2013), various S species were grouped as three oxidation state, including reduced (peak energy < 2475 eV and oxidation number -2 ~ +0.5), intermediate (peak energy 2475 - 2479 eV and oxidation number +2 ~ +3.68) and oxidized (peak energy > 2480 eV and oxidation number +4 ~ +6) because it was difficult to determine one by one soil S species. According to visual observations, the peak intensity of intermediate S in FM soils is greater than NK soils, and these were changed during the soil incubation period.

Fig. S4. Sulfur K-edge XANES spectra of soil samples (circles) and their LCF using the reference spectra (solid lines).

Table S1. The best and second-best (in parentheses) results of LCF on Cd K-edge EXAFS spectra of soil samples

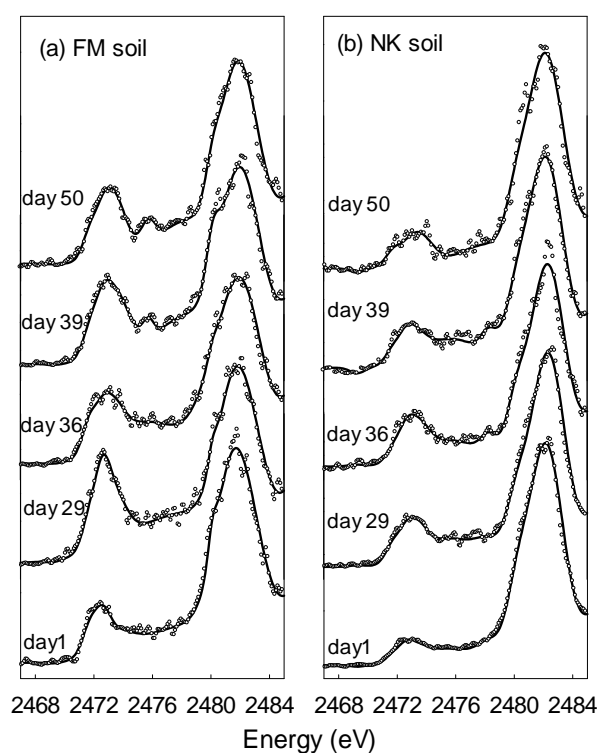| Time	Cd-ferrihydrite	Cd-humus	CdS	CdCl$_2$	R †
		-------------------------------------%-------------------------------------			
		FM soil			
Day 1	65	35			0.123
	(90)			(10)	(0.127)
Day 4	73		27		0.135
		(67)	(33)		(0.149)
Day 19			85	15	0.107
	(8)		(92)		(0.118)
Day 29			93	7	0.115
	(6)		(94)		(0.116)
Day 34			89	11	0.064
	(12)		(88)		(0.067)
Day 36			74	26	0.119
	(36)		(64)		(0.121)
Day 39		65	35		0.102
	(69)		(31)		(0.106)
Day 41	81		19		0.104
		(79)	(21)		(0.107)
Day 50		84	16		0.102
	(85)		(15)		(0.102)
		NK soil			
Day 1		87		13	0.073
	(33)	(67)			(0.078)
Day 4		82		18	0.140
	(41)	(59)			(0.147)
Day 19		73	27		0.113
	(76)		(24)		(0.116)
Day 29	67		33		0.163
			(50)	(50)	(0.167)
Day 34	64		36		0.088
		(60)	(40)		(0.089)
Day 36	63		37		0.100
		(58)	(42)		(0.104)
Day 39	40		60		0.072
		(33)	(67)		(0.078)
Day 41		84	16		0.086
	(85)		(15)		(0.089)
Day 45	84		16		0.091
		(81)	(19)		(0.098)
Day 50	80		20		0.080
		(77)	(23)		(0.084)

† R: residual value for fitting; $R = \Sigma(\mu_{exp} - \mu_{model})^2 / \Sigma(\mu_{exp})^2$

Table S2   The best and second-best (in parentheses) results of LCF on Cd K-edge XANES spectra of soil samples

Time	Cd-ferrihydrite	Cd-humus	Cd-gibbsite	Cd-birnessite	Cd-kaolinite	CdS	CdCl$_2$	CdCO$_3$	Cd(OH)$_2$	R (10^{-4})†
				--%--						
				FM soil						
Day 1		85				15				2.64
		(73)							(28)	(3.71)
Day4‡		57				43				1.57
Day 19					13	87				3.92
						(91)			(9)	(4.20)
Day 29					11	89				4.74
						(92)			(8)	(4.92)
Day 35					22	78				3.10
						(83)			(17)	(3.88)
Day 36					37	63				1.47
					(31)	(69)				(2.84)
Day 39					70	30				2.93
					(61)	(39)				(3.94)
Day 41		71				29				2.51
		(64)					(36)			(7.91)
Day 50		72				28				2.43
		(64)					(37)			(5.90)
				NK soil						
Day 1	41	59								1.12
		(57)	(43)							(1.95)
Day 4		81				19				1.26
		(78)							(22)	(4.17)
Day 19‡		60				40				11.6
Day 29‡		51				49				7.46
Day 35‡		53				48				6.76
Day 36		52				48				2.14
					(42)	(58)				(10.2)
Day 39‡				55		45				7.68
Day 41					73	28				2.84
		(56)					(44)			(3.77)
Day 45		65					35			3.34
		(78)					(22)			(5.49)
Day 50		61					39			3.61
						(67)	(34)			(5.08)

† R: residual value for fitting; $R = \Sigma(\mu_{exp} - \mu_{model})^2 / \Sigma(\mu_{exp})^2$
‡ The results of second-best fit were not shown due to poor fit (R value) with one order different from that of the best fit.

References

Hashimoto, Y. and N. Yamaguchi. 2013. Chemical Speciation of Cadmium and Sulfur K-Edge XANES Spectroscopy in Flooded Paddy Soils Amended with Zerovalent Iron. Soil Sci. Soc. Am. J. 77: 1189-1198. doi:10.2136/sssaj2013.01.0038.

Lindsay, W.L. 1979. Chemical Equilibria in Soils. John Wiley, New York, NY.